IAA-AAS-DyCoSS1 -08-08

A NOTE ON THE DYNAMICS AROUND THE $L_{1,2}$ LAGRANGE POINTS OF THE EARTH–MOON SYSTEM IN A COMPLETE SOLAR SYSTEM MODEL

Lian Yijun[*], Gerard Gómez[†], Josep J. Masdemont[‡], Tang Guojian[§]

In this paper we study the dynamics of a massless particle around the $L_{1,2}$ libration points of the Earth-Moon system in a full Solar System gravitational model. The study is based on the analysis of both the periodic and quasi-periodic solutions around the two collinear equilibrium points, whose computation is implemented using as initial seeds the libration point orbits of Circular Restricted Three Body Problem, determined by Lindstedt-Poincaré methods. In order to do these analysis, an effective algorithm is proposed which, being capable of refining large time-span libration point orbits in real ephemeris, is an iterative combination of a multiple shooting method with a detailed Fourier analysis of the orbits computed with the multiple shooting.

INTRODUCTION

The purpose of this paper is the study of the phase space around the collinear libration points L_1 and L_2 of the Earth–Moon system when the gravitational effects of the remaining bodies of the Solar System are taken into account. In the simplified model defined by the Circular Restricted Three Body Problem (CR3BP), the description of the phase space around these two points has already been done in the past, either using semi-analytical techniques[1] or numerical ones.[2] When using more realistic models of motion, the refinement of the different kinds of libration point orbits around both points (see Gómez *et al.*[3]) has some problems when the time interval used is large. These problems are more evident for the Earth–Moon L_2 point due to a 1:2 resonance between the natural frequency of some halo orbits (ω_h) and the external frequency due to the perturbation of the Sun (ω_s); in fact $\omega_h \simeq 2\omega_s$ for some orbits of the halo family of periodic orbits around this point. To analyse more closely this fact, Andreu[4] introduced an intermediate model between the CR3BP and the restricted n-body problem, which is the so called Quasi-Bicircular Problem. It is a restricted four body problem in which the three primaries move following a "true" solution of the three body problem along orbits close to circular (the Earth and the Moon around their barycenter, and the Earth-Moon barycenter around the Sun). The description of the different types of orbits in the neighbourhood of L_2 is also done in Reference 4 by means of the reduction of the Hamiltonian of the problem to the central manifold. The reduced Hamiltonian is then studied by means of Poincaré maps at different energy levels.

[*]College of Aerospace and Material Engineering, National University of Defence Technology, 410073 Changsha, China & Departament de Matemàtica Aplicada i Anàlisi, Universitat de Barcelona, Gran Via 585, 08007, Spain
[†]IEEC & Departament de Matemàtica Aplicada i Anàlisi, Universitat de Barcelona, Gran Via 585, 08007 Barcelona, Spain
[‡]IEEC & Departament de Matemàtica Aplicada I, ETSEIB, Universitat Politècnica de Catalunya, Diagonal 647, 08028 Barcelona, Spain
[§]College of Aerospace and Material Engineering, National University of Defence Technology, 410073 Changsha, China.

In this paper, using as gravitational model the restricted n-body problem and taking as primaries the Solar System bodies (SSRnBP), we will compute a large set of libration orbits around the dynamical substitutes for this model of the two libration points. For this purpose it has been necessary to develop a numerical procedure that, starting with orbits computed in the CR3BP, does their numerical refinements in the SSRnBP for large time intervals (of around 60 years, which covers most of the relevant Sun-Earth-Moon periods). The method is an iterative one, combination of a multiple shooting method and a refined Fourier analysis of the orbits obtained with the shooting procedure. This combination allows for the determination of accurate seeds when increasing the length of the time interval in the shooting method.

The paper has been organised as follows: in the first section we explain the refinement procedure and some details about its implementation. The next section is devoted to the dynamical substitutes of the libration points L_1 and L_2 and illustrates the numerical method used. In the next two sections the results obtained for the periodic and Lissajous orbits are given. These results are summarised using a Poincarè map representation for the orbits obtained. Finally, in the last section some conclusions about the results obtained are given.

THE NUMERICAL REFINEMENT PROCEDURE

The purpose of this section is to explain the procedure that has been developed to get solutions of more realistic equations, for the description of the motion in the Earth-Moon neighbourhood, that remain close to the solutions obtained for the CR3BP. As mentioned in the Introduction, the model equations that will be used for the refinement are Newton equations for the restricted n-body problem (SSRnBP), using some JPL ephemeris data file for the determination of the states of the Solar System bodies.

An important restriction of the method, considering that we are going to compute orbits numerically, is that a specific time span must be fixed, which means an initial epoch (since the new differential equations are non-autonomous) and the length of the time span. With the computed orbits, that will cover a considerably large time interval (up to 60 years), it will be possible to detect long-term dynamical properties of the gravity field under consideration.

Main functional components of the algorithm

The algorithm for the numerical refinement has three main components: an initial seed for the multiple shooting procedure, a multiple shooting procedure, and a refined Fourier analysis method.

In the proposed algorithm, the simple CR3BP model is used to provide an initial seed for the shooting procedure. As is well known, using adimensional units (AU) the equations of CR3BP are (see Szebehely[5]):

$$\ddot{x} - 2\dot{y} = \Omega_x, \ddot{y} + 2\dot{x} = \Omega_y, \ddot{z} = \Omega_z, \tag{1}$$

where

$$\Omega = \frac{1}{2}(x^2 + y^2) + \frac{1-\mu}{r_1} + \frac{\mu}{r_2} + \frac{1}{2}\mu(1-\mu),$$

and $r_1 = \sqrt{(x-\mu)^2 + y^2 + z^2}$, $r_2 = \sqrt{(x-\mu+1)^2 + y^2 + z^2}$ are the distances from the particle to the two primaries. Note that the above equations are given in a rotating frame, with the x-axis pointing from the small primary to the big one. All the plots in this paper will use this same reference frame and adimensional units unless indicated otherwise. The above system of differential equations

has a first integral called the Jacobi integral, which is defined as

$$C_J = 2\Omega - \dot{x}^2 - \dot{y}^2 - \dot{z}^2. \tag{2}$$

The Jacobi Constant C_J is associated with the energy of the system.

As is discussed in References 1 and 2, various families of bounded orbits exist in the CR3BP, among which the planar and vertical Lyapunov periodic orbits, halo, quasi-halo and Lissajous orbits are the typical ones. In the framework of the CR3BP, these orbits can be computed in both analytical and numerical ways. Their analytical expansions, using Lindstedt-Poincaré methods up to high order, give good approximations, as can be shown when comparing them against the numerically determined trajectories during a certain time interval. The expansions loose convergence at energy levels far from the one corresponding to the equilibrium point or if the orbits are too large, which usually are not very useful for practical applications. For the computation of the initial seed of the procedure, we will use libration point orbits determined by means of their Lindstedt-Poincaré expansions, so our explorations will have the two constraints just mentioned. After the first iteration of the algorithm, the seed for the multiple shooting will be determined using the results of the Fourier analysis, as is explained below.

The parallel shooting algorithm that has been implemented follows closely the one described in Reference 3. The result of the procedure is essentially a series of states (nodes) along the refined trajectory. When numerically integrating these nodes, the matching errors in position and velocity are small (less than $1mm$ in position and $0.1mm/day$ in velocity throughout this work) for the orbit to be viewed as a continuous one. Taking as initial seed the nodes, equally or unequally spaced in time along a libration point orbit, the algorithm solves the matching equations using a modified Newton method, in which the norm of the correction is minimised at each step; in this way the linear system that must be solved for the computation of the corrections is well conditioned. For large time spans, the convergence of the multiple shooting strongly depends on the accuracy of the initial guess as a "solution" of the SSRnBP.

The last component of the method is the refined Fourier analysis procedure described in References 6, 7. This method is essentially a collocation method for solving the following problem: given N_f samples $\{f(jT/N_f)\}_{j=0}^{N_f-1}$ of a real-valued quasi-periodic function $f(t)$, equally spaced in $[0, T]$, determine a trigonometric polynomial,

$$Q_f(t) = A_0^c + \sum_{l=1}^{N_f} \left[A_l^c \cos(\omega_l t) + A_l^s \sin(\omega_l t)\right] \tag{3}$$

whose frequencies $\{\omega_l\}_{l=1}^{N_f}$, and amplitudes, $\{A_l^c\}_{l=0}^{N_f}$, $\{A_l^s\}_{l=1}^{N_f}$, are a good approximation of the ones of $f(t)$. For our problem, the Fourier analysis is done to the three time series associated to the coordinates $(x(t), y(t), z(t))$ of the trajectory determined by the multiple shooting.

The trigonometric approximations of the orbits obtained at a given step are used to compute new guessed nodes in a longer time interval for the next step of the shooting. It will be shown that, along the iterations, the set of basic frequencies determined by the Fourier analysis (all the frequencies will be linear combinations of the basic ones) tend to be constant. With the iterations of the refinement procedure, the length of the time interval will be enlarged by, for instance, adding a constant quantity or multiplying the previous length by a constant amount.

The algorithm

As has been said, the whole procedure is an iterative process invoking the three main functional components introduced above. A more detailed description requires the introduction of some notation. Let T_0 be the initial epoch, which should be fixed due to the non-autonomous nature of SSRnBP, ΔT the time-span covered by a certain set of nodes, ΔT_0 the time-span of the initial guess provided by the CR3BP, and ΔT^* the desired final time-span we want to achieve. During the process, either a ratio γ_P is used to enlarge ΔT at each step ($\Delta T = \gamma_P \Delta T$) or a constant time step δT is added to the previous one ($\Delta T = \Delta T + \delta T$). Since the former way needs less steps to reach a given time span, it has been the one mainly used through this paper. Typical values used for these quantities are: $T_0 = J2000.0$, $\Delta T_0 = 400$ *adimensional time units* (TU), $\Delta T^* = 60$ years, and $\gamma_P = 1.3$.

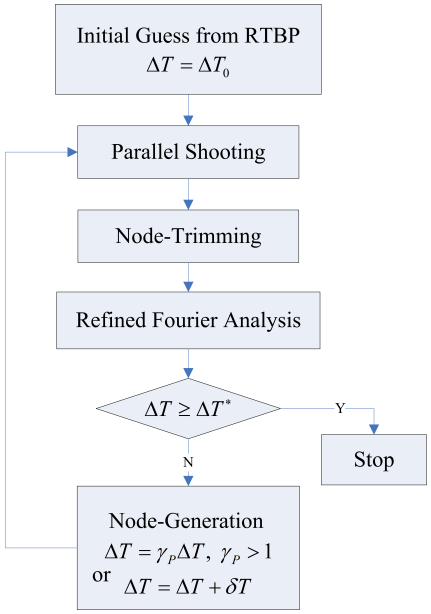

Figure 1. The basic procedure of the proposed algorithm for refining orbits of large time span in real ephemeris.

The procedure, whose flow chart is shown in Figure 1, has been implemented according to the following steps:

Algorithm

Step 1: Generate nodes from CR3BP as an initial guess for *Step* 2;

Step 2: Fixing a certain epoch T_0, perform the parallel shooting with the initial guess;

Step 3: Trim a certain number of the nodes obtained from *Step* 2 to cope with the fact that no boundary conditions are required in the multiple shooting method;

Step 4: Do the refined Fourier analysis of the three state components of the orbit computed in *Step* 3. The output of the analysis will be a set of basic frequencies and the associated amplitudes of the trigonometric approximation of the orbit;

Step 5: Check the total time-span condition: if $\Delta T \geqslant \Delta T^*$, go to *Step* 7, otherwise, go to *Step* 6;

Step 6: Compute the new nodes as initial guess for a larger time-span $\Delta T = \gamma_P \Delta T, \gamma_P > 1$, using the trigonometric approximations of the coordinates computed in *Step* 4; then go to *Step* 2;

Step 7: Stop.

Note that *Step* 3 is required before proceeding to *Step* 4. Since no boundary conditions are imposed in the multiple shooting method, the two end segments of the resulting orbit are usually far from the periodic or quasi-periodic initial approximation, and usually follow the natural dynamics of the problem which has a dominant unstable component. Removing the nodes associated with these two end segments we are closer to the desired final quasi-periodic orbit, so that the determination of trigonometric approximations for their coordinates makes sense. Usually, for libration point orbits of the Earth–Moon system, it is sufficient to trim the nodes for half a month at both ends.

Another point worth to mention is the maximum number of frequencies to be determined in *Step* 4, which plays an essential role in the accuracy of the Fourier analysis, as well as in the determination of the basic frequencies. If it is too small, the nodes computed in *Step* 6 will be poor approximations of the true orbit with the associated convergence problems in the parallel shooting process. On the other hand, if it is too big, the computational time spent on the refined Fourier analysis and the determination of an initial guess will be longer. Furthermore, in this case, the Fourier analysis will end up with much fewer frequencies under a given required accuracy when the time span of the orbit is not very large (not many frequencies have appeared). The value we have chosen for this study is 6 when the time span is lower than 2000TU (around 23.5 years), and 20 otherwise.

Parallel implementation

In the proposed algorithm, the parallel shooting is the critical part in terms of computational time. Using our testing machine (Intel Core i3 CPU M330 2.13GHz, 2GB, 4 cores), for one iteration, the computational time is approximately 19 seconds for a Lissajous orbit with 50000 nodes, while a successful refinement usually requires 10 to 15 iterations, which makes it rather time-consuming if there are many orbits to explore.

In each iteration, the core procedure of the parallel shooting involves three consecutive steps, i.e., (1) numerically integrating each node of the initial guess using JPL ephemeris, (2) padding a Jacobian matrix, and (3) determining the corrections, respectively. The first two steps are the most time-consuming part of the routine due to their node-by-node nature which, consequently, ought to be the target of parallelism implementations. In order to speed up the shooting, we have used OpenMP® * as our tool, which is an Application Program Interface (API) that may be used to explicitly direct multi-threaded, shared memory parallelism, providing the capability to implement both coarse-grain and fine-grain ones. The API supports C/C++ and FORTRAN on a wide variety of architectures. By adapting OpenMP to our FORTRAN code, the time cost for the same calculation is decreased to around 7 seconds. The computational time is reduced when the code is transferred to a machine with more cores.

DYNAMICAL SUBSTITUTES OF THE $L_{1,2}$ LIBRATION POINTS

Before studying the neighbourhood of the L_1 and L_2 equilibrium points, we will first compute the dynamical substitutes of both points in the SSRnBP. With the proposed methodology, the time spans for both cases have been extended up to 100 years.

*openmp.org/wp/

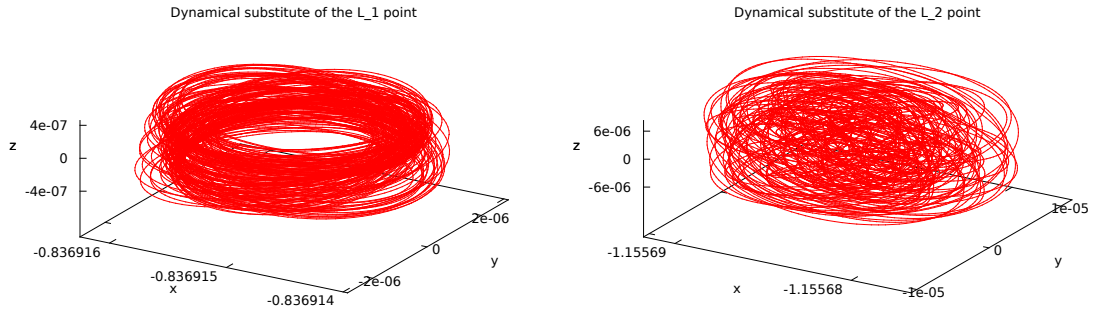

Figure 2. Dynamical substitutes in the SSRnBP of the L_1 and L_2 points of the Earth–Moon system computed for a 5-year time span.

The initial seeds for the procedure are just the two equilibrium points. The initial total time interval has been of 5 years and a value of $\gamma_P = 1.2$ has been used to reach the maximum value $\Delta T^* = 100$ years. The resulting orbits are shown in Figure 2 for a 5-year time interval. The 100 years orbits have almost the same size and shape as the ones displayed. For this time interval, the intersections of both orbits with the $z = 0$ plane is shown in Figure 3.

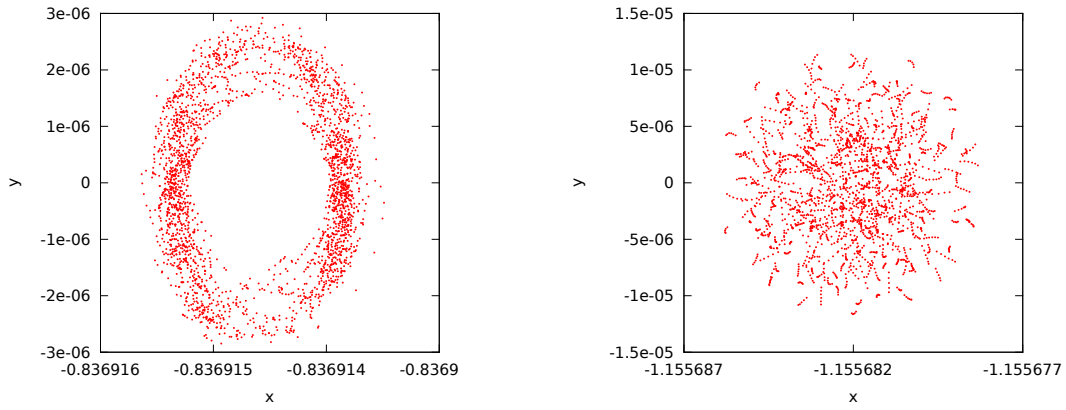

Figure 3. Poincaré map representation of the dynamical substitutes of the L_1 (left) and L_2 (right) points for 100 years in the SSRnBP.

For both equilibrium points, using the frequencies obtained from the Fourier analysis, one can determine a reduced set of basic frequencies. Once they have been determined, all the frequencies resulting from the Fourier analysis can be written as integer linear combinations of these basic ones. In Figure 4 we show the evolution, with respect the total time interval, of the three basic frequencies associated to the two equilibrium points. As it can be seen, their values (as well as the associated amplitudes, that are not displayed) tend to constant values. This means that the numerical procedure implemented, when seen as a dynamical system, has these two orbits as fixed points: they are the dynamical substitutes of the two libration points. These results are in complete agreement with those obtained by other methods in Gómez *et al.*[8] and Hou *et al.*[9] As can be seen from the figures, the sizes of both orbits are quite small (on the order of $1.0E{-}6$ adimensional units, around $0.38km$ for L_1, and $1.0E{-}5$ adimensional units, around $3.8km$ for L_2). Although its size is smaller, the

trajectory of L_1 moves in a more regular way than the one of L_2, which tries to fill up the space it subsists. This fact partially reflects the rich dynamics around Earth–Moon L_2 point.

Recall that a set of basic frequencies is determined up to an unimodular linear transformation. In our case, the frequencies that have been taken as basic can also be written (using an unimodular transformation) in terms of the basic frequencies of the motion of the Moon (see Escobal[10]) and the frequencies associated with the two purely imaginary eigenvalues of the linear part of the CR3BP vector-field at the equilibrium points which, according to Lyapunov theorem, are associated to the two Lyapunov families of periodic orbits which emanate from them.

NUMERICAL REFINEMENT OF PERIODIC ORBITS

This section is devoted to the refinement of periodic orbits around both L_1 and L_2, which include the planar and vertical Lyapunov orbits, and the halo ones. Since they are periodic, only one frequency exists for them.

The planar and vertical Lyapunov families around L_1 and L_2

At each energy level, the Lyapunov family is closely associated with the Lissajous one in the sense that the former confines the latter in phase space for a given energy level. The planar Lyapunov orbit is located at the x–y plane, giving an in-plane motion boundary to the Lissajous orbits (see Figures 14 and 15). The vertical Lyapunov orbit, which has zero in-plane motion, sets an out-of-plane limit for the Lissajous ones.

For either of the two Lyapunov families, different energy levels will result in orbits with different sizes. The values of the Jacobi constant we choose for this Section are 3.186, 3.194, and 3.200 for L_1, and 3.162, 3.174, and 3.184 for L_2. In Figures 5 and 6, we present refinements of the planar Lyapunov orbits and the vertical Lyapunov ones, respectively, with respect to the selected energy levels for both L_1 and L_2. Only the first 3 years of the 60-year refinement are plotted for each orbit. For comparison, orbits in CR3BP are also displayed in both figures. In Figure 5, one can see that, due to the perturbation of the Sun, the refinements of the planar Lyapunov orbits are no longer two dimensional; they obtain a small amplitude for vertical motion along the z-direction. Also note that the orbits, whose energy levels ($C_J = 3.200$ for L_1, and $C_J = 3.184$ for L_2) are very close to the ones of the equilibrium points ($C_J^{L_1} = 3.200344$ and $C_J^{L_2} = 3.184163$), have tiny sizes compared with the others. Lastly, the refined orbits of both families are all quasi-periodic, but the baseline shapes and sizes have sustained.

The halo families around L_1 and L_2

Due to the symmetry of the problem with respect to the x–y plane, in the CR3BP there are two families of halo orbits. In this paper, we have refined orbits of the family that have their maximum z-amplitude along the positive z direction.

Halo orbits in CR3BP are characterised by one amplitude parameter, β, in the z direction, which describes the size of the orbit. Different values of β are associated with different Jacobi constants and periods in a monotonical way (see Figure 7). In other words, given any one of these three parameters, one particular halo orbit is specified. The β values used in this section vary within the interval 0.03–0.48 with a step size of 0.03, for both L_1 and L_2. The total time span is $\Delta T^* = 60$ years, and only the first 3 years of the four refined orbits ($\beta = 0.12, 0.24, 0.36, 0.48$) are displayed in Figures 8 and 9. For comparison, orbits in CR3BP are also shown in these two figures. As can

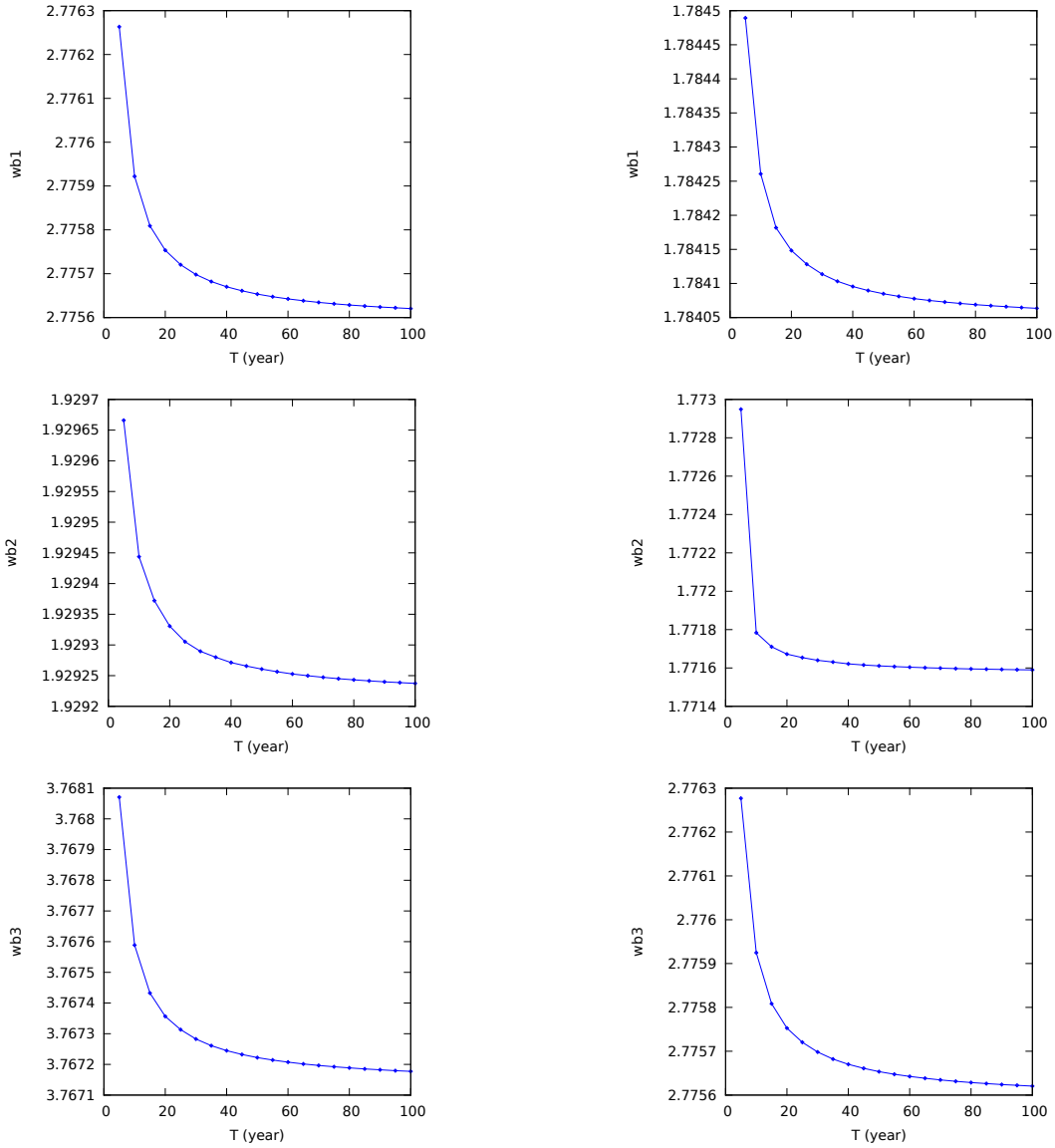

Figure 4. The first three basic frequencies of the dynamical substitutes of L_1 point (left hand side column) and L_2 point (right hand side column) with respect to different time spans.

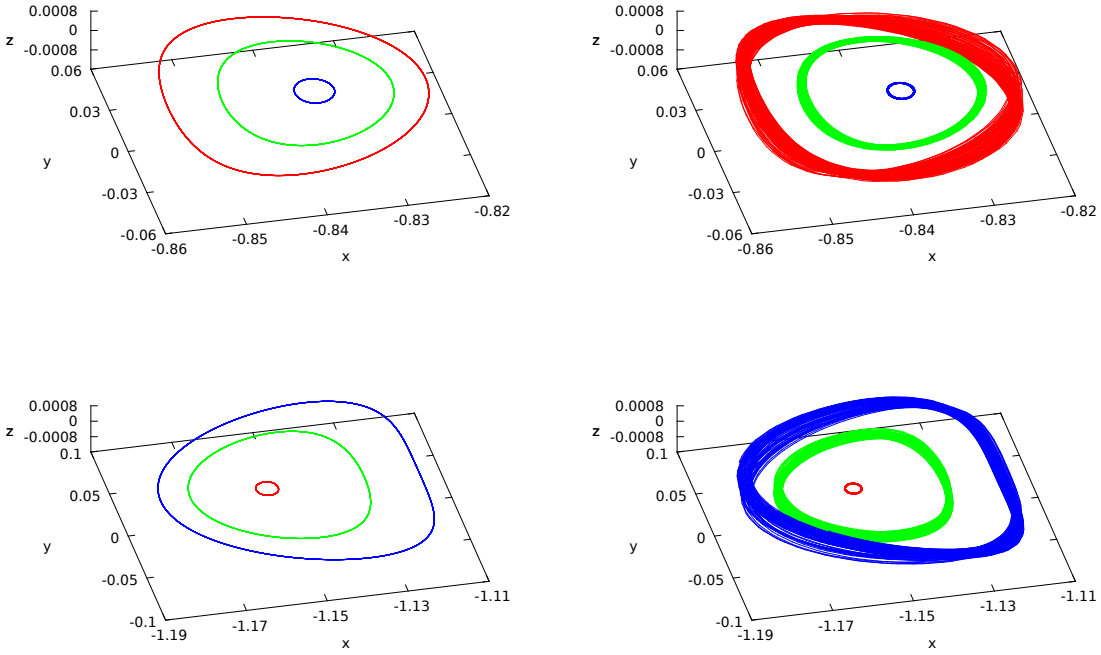

Figure 5. Planar Lyapunov orbit refinements for both L_1 (top) and L_2 (bottom). Only the first 3 years of the 60-year orbits are plotted here. On the left hand side are the orbits in CR3BP, on the right hand side the refinements in SSRnBP. The values of C_J are 3.186 (largest orbit), 3.194 and 3.200 (smallest orbit) for L_1, and 3.162 (largest orbit), 3.174, and 3.184 (smallest orbit) for L_2.

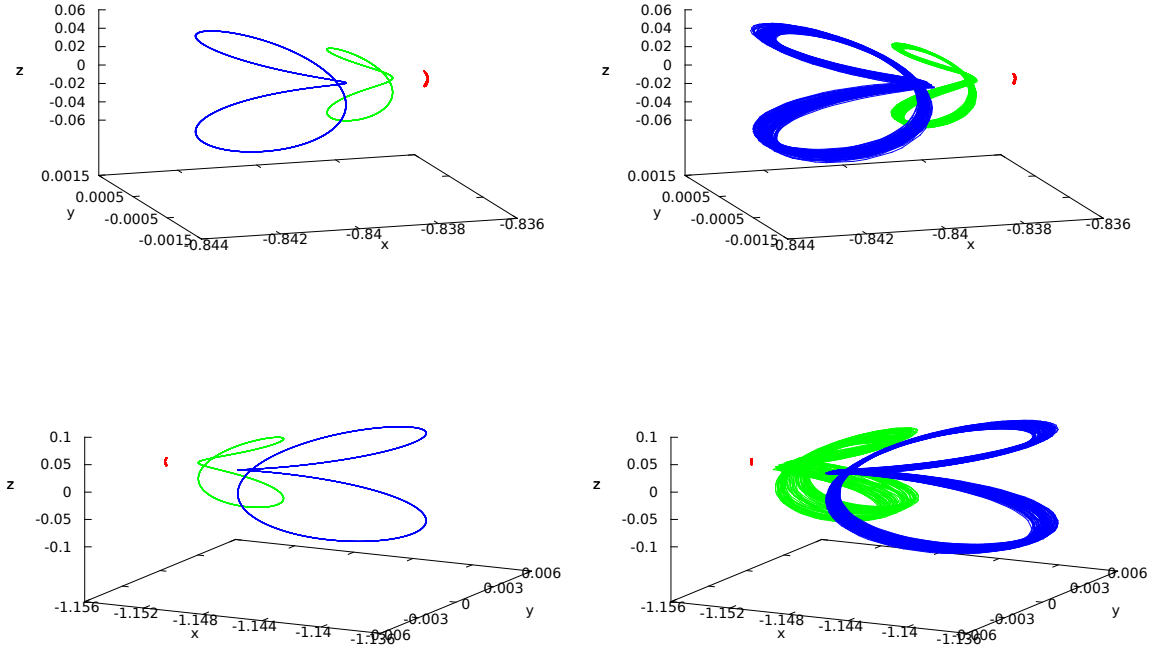

Figure 6. Vertical Lyapunov orbit refinements for both L_1 (top) and L_2 (bottom). Only the first 3 years of the 60-year orbits are plotted here. On the left hand side are the orbits in CR3BP, on the right hand side the refinements in SSRnBP. The values of Jacobi Constant are 3.186 (largest orbit), 3.194 and 3.200 (smallest orbit) for L_1, and 3.162 (largest orbit), 3.174, and 3.184 (smallest orbit) for L_2.

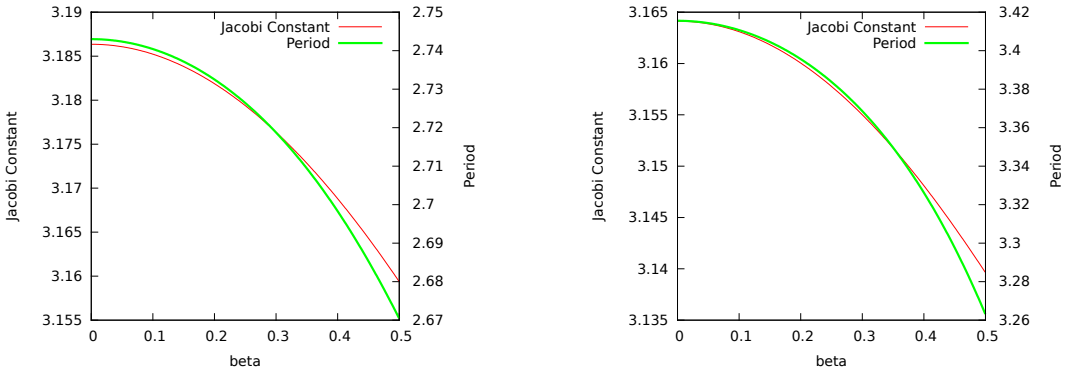

Figure 7. Jacobi Constant and Period vs β for both L_1 (left) and L_2 (right) halo orbits in CR3BP model.

be seen, the refinement of halo orbits produces a quasi-periodic one, but for most of the orbits the baseline shape and size do not change.

Note that NOT all the refinements of halo orbits are able to sustain the basic shape as in CR3BP. Those with small values of β (less than 0.1) will loose the geometry during the refining process, due to the strong gravitational disturbances near the x–y plane, and will eventually evolve to orbits similar to the refinement of a planar Lyapunov one.

Special attention should be paid to some L_2 halo orbits, at which the proposed algorithm encounters difficulties. As seen in Figure 10, there is a gap between the two segments of the basic frequencies. Actually, it is where the 1:2 resonance, between the basic frequency of the halo orbit ($\omega_h \simeq 1.850$) and the one due to the perturbation of the Sun ($\omega_s \simeq 0.925196$), occurs as mentioned in the Introduction. In this case, the proposed algorithm is unable to refine the orbits for $\Delta T^* = 60$ years, although we have been able to do their refinement up to $\Delta T^* = 25$ years.

NUMERICAL REFINEMENT OF LISSAJOUS ORBITS

This section deals with the refinement of Lissajous orbits for a large time span (up to 60 years). Unlike the periodic orbits in CR3BP which have only one frequency, Lissajous orbits are quasi-periodic orbits characterised by two frequencies.

Lissajous orbits are parameterised by two amplitudes in the Lindstedt-Poincaré (LP) expansions, which are the in-plane amplitude (α) and the out-of-plane amplitude(β). These two parameters are correlated with each other on a specific energy level, that is, given a Jacobi constant value, if one amplitude is fixed, the other will be uniquely determined. This correspondence should behave monotonically (see Figure 11) if the LP series are within their radius of convergence. Note that (0–β) corresponds to the vertical Lyapunov family, and (α–0) the planar Lyapunov one. As is seen in Figure 11, those L_2 Lissajous orbits, which are of the same amplitudes as the L_1 ones, will possess a higher energy level. In terms of Jacobi constant, the valid range of the LP expansions, which holds the monotonic relation between α and β, will be between 3.186–3.200 for L_1, and 3.162–3.184 for L_2.

For each pair of (α–β), or a given Lissajous orbit, there are two basic frequencies in response, one of which is the in-plane frequency (ω_1) and the other the out-of-plane frequency (ω_2). The relation

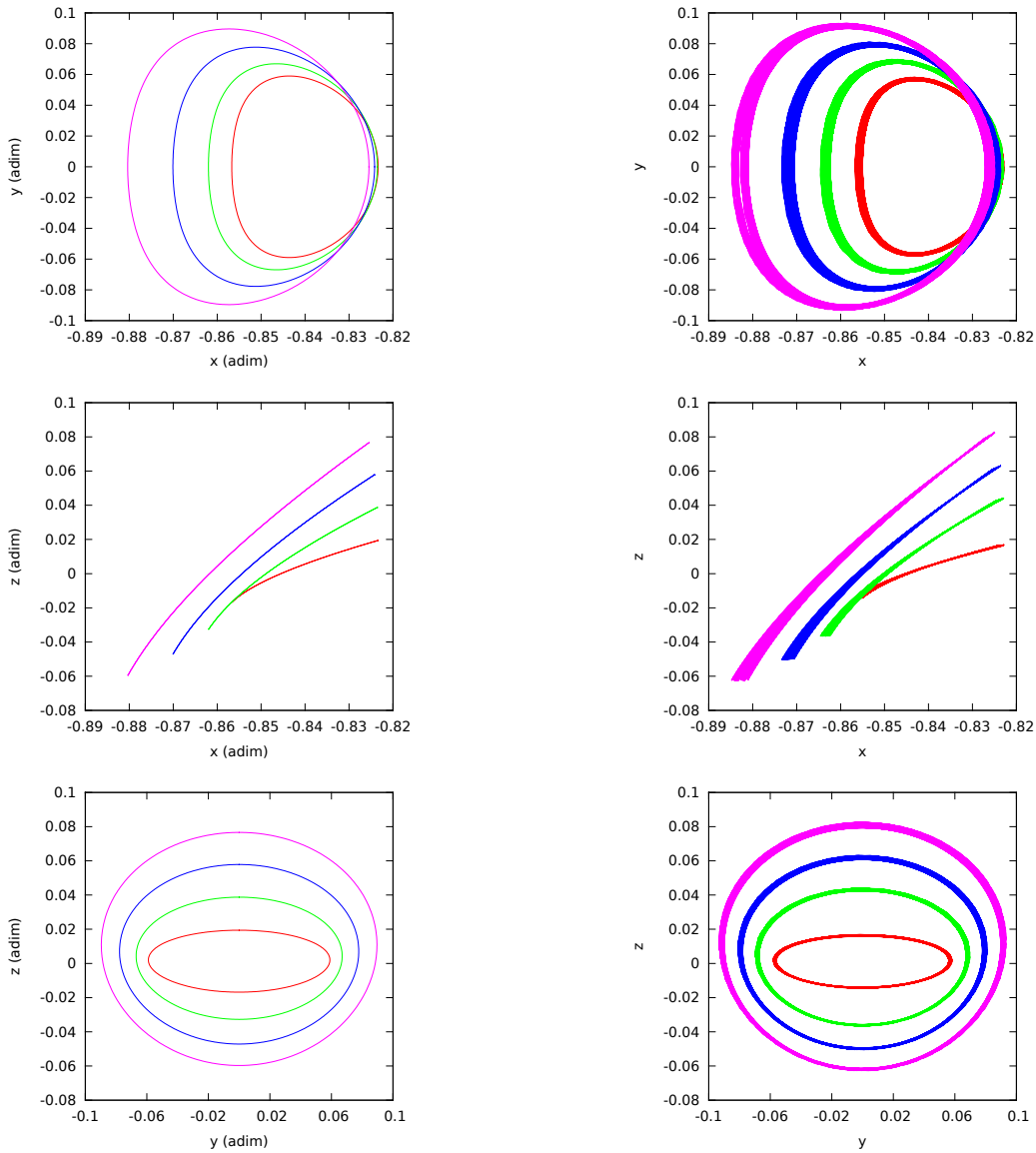

Figure 8. The initial guess from CR3BP (left) and refinement (right) of halo orbits with $\beta = 0.12$ (smallest orbit), 0.24, 0.36, 0.48 (largest orbit) of the Earth–Moon L_1 point. The orbits have been refined for 60 years, but only the first 3 years are plotted here.

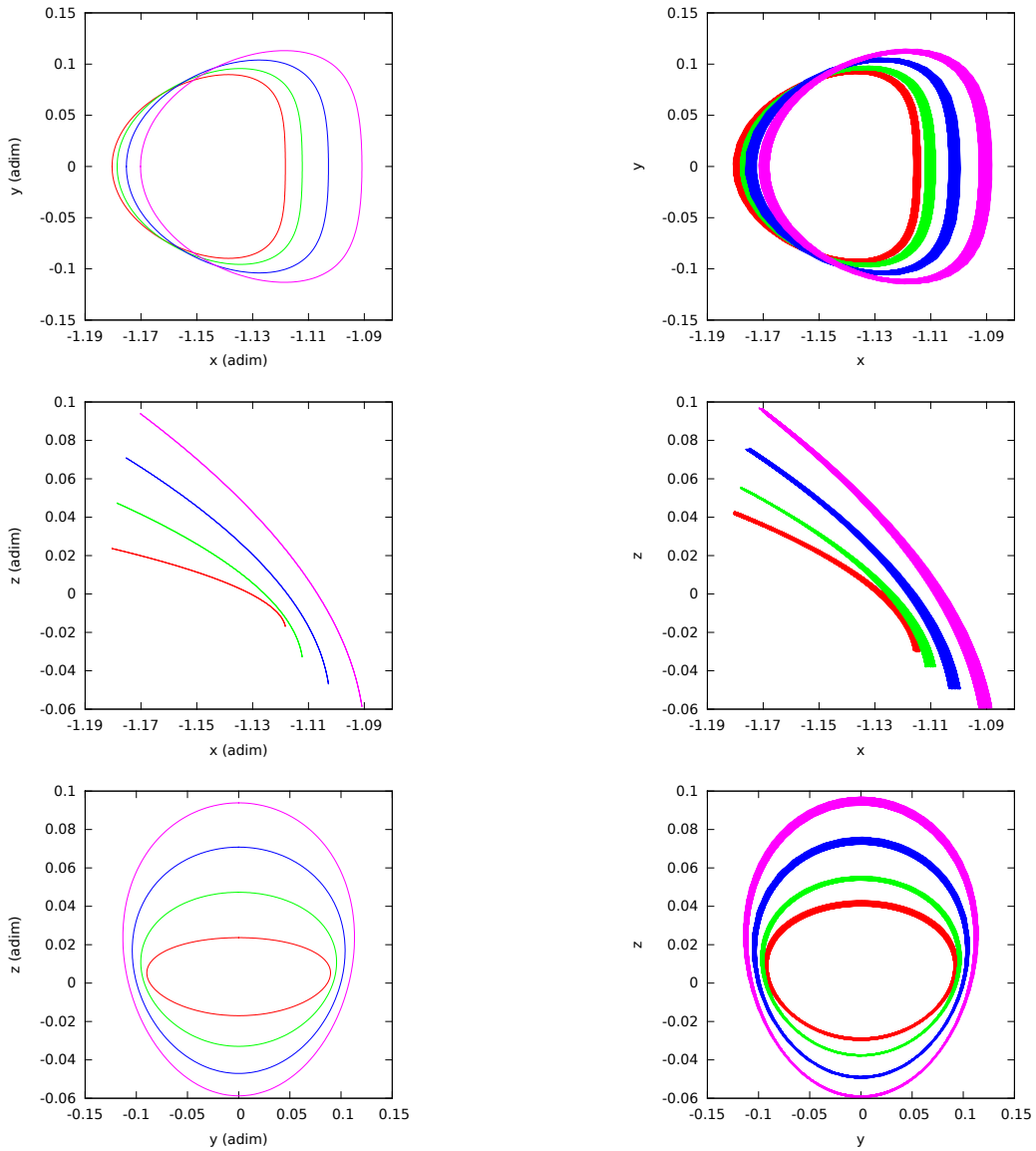

Figure 9. The initial guess from CR3BP (left) and refinement (right) of halo orbits with $\beta = 0.12$ (smallest orbit), 0.24, 0.36, 0.48 (largest orbit) of the Earth–Moon L_2 point. The orbits have been refined for 60 years, but only the first 3 years are plotted here.

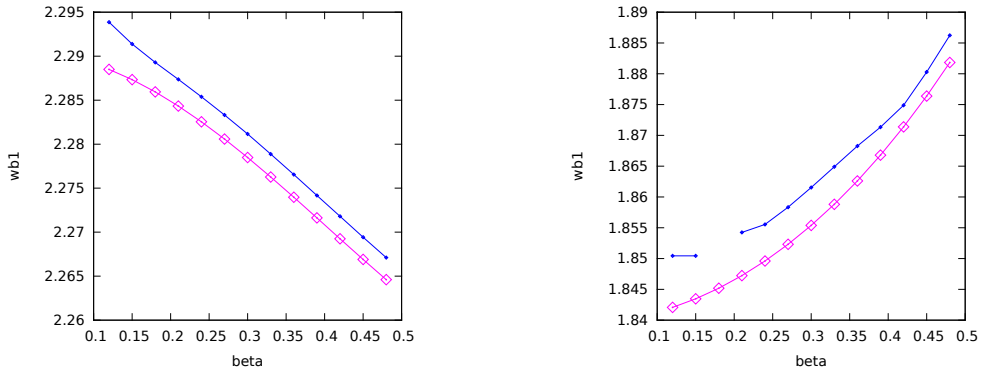

Figure 10. The first basic frequencies of the halo orbits of L_1 point (left) and L_2 point (right) with respect to β. The curve with $\boxdot$ represents the frequencies of halo orbits in CR3BP, and the other one shows the first basic frequencies resultant from the refined Fourier analysis.

between these two frequencies, with respect to different values of Jacobi Constant (energy level), are displayed in Figure 12.

In Figure 13, we give an example of the 60-year refinement of a Lissajous orbit around L_1, whose parameters in CR3BP are $\alpha = 0.0579999987$ and $\beta = 0.1285250065$, corresponding to an energy level of $C_J = 3.194$. Due to the large number of nodes for 60 years, only the leg of the first 10 years is plotted. The rest part of the orbit simply fill up the torus in a denser way. In this figure, one can easily see some near resonance happens, which will be further revealed and discussed in the following section.

A POINCARÉ MAP REPRESENTATION OF THE PHASE SPACE AROUND $L_{1,2}$

In this section, we present Poincaré maps, with $\{z = 0, \dot{z} > 0\}$, of Lissajous orbits and Lyapunov ones in CR3BP and their refinements in SSRnBP for both L_1 and L_2. To depict the phase space in a coherent way, we require the intersections (CR3BP model) on the same plot to share the same Jacobi Constant. The selected Jacobi constant values for the orbits around L_1 are 3.188, 3.194, and 3.200, and 3.166, 3.174, and 3.184 for those around L_2. Results are shown in Figures 14 and 15 for L_1 and L_2, respectively, where on the left hand side are the Poincaré intersections of orbits in CR3BP and on the right hand side the corresponding refinements in SSRnBP for 60 years.

In both Figures 14 and 15, in each plot on the left column (CR3BP case), the most outer intersection is actually the entire planar Lyapunov orbit on that energy level, while in the middle there exists a fixed point, which represents a vertical Lyapunov orbit. When having been refined for 60 years in SSRnBP (on the right hand side column), the locations and geometries of their intersections do not change much, except for the case in which the energy level is very close to the one of equilibrium point (see the $C_J = 3.200$ case in Figure 14 and $C_J = 3.184$ case in Figure 15).

As for Lissajous orbits, more dynamical phenomenons appear. In Figure 14, one can see some near resonance happens to the refinement of two non-resonant orbits in CR3BP, which are next to the outermost ones at $C_J = 3.188$ and 3.194. This means that long-term dynamical properties can be altered by the perturbation of the Sun. In fact, resonance can also happen to the refinement of L_2 Lissajous orbits at some energy level (not to the ones shown in Figure15). Another fact worth to

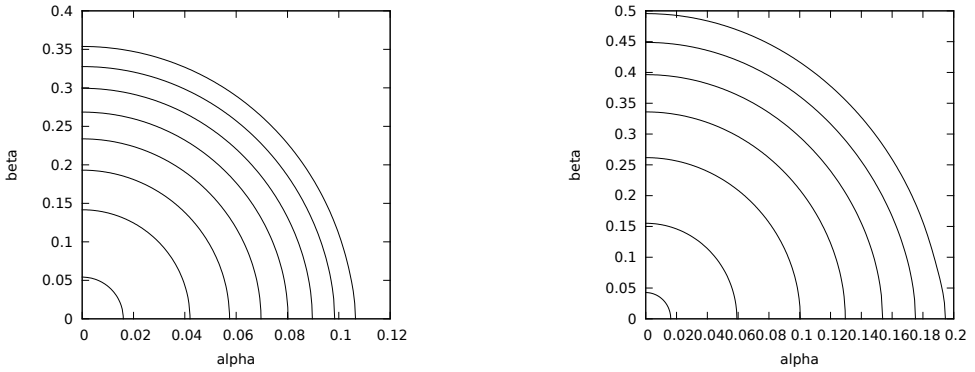

Figure 11. The monotonic relation between in-plane amplitude (α) and out-off-plane amplitude (β) of Lissajous orbits for Earth–Moon L_1 point (left) and L_2 (right). For the L_1 plot, the Jacobi Constant values are 3.186 (outer curve)–3.200 (inner curve) with a 0.002 step size. For the L_2 plot, the Jacobi Constant values are 3.162 (outer curve)–3.182 with a 0.004 step size, and 3.184 (inner curve).

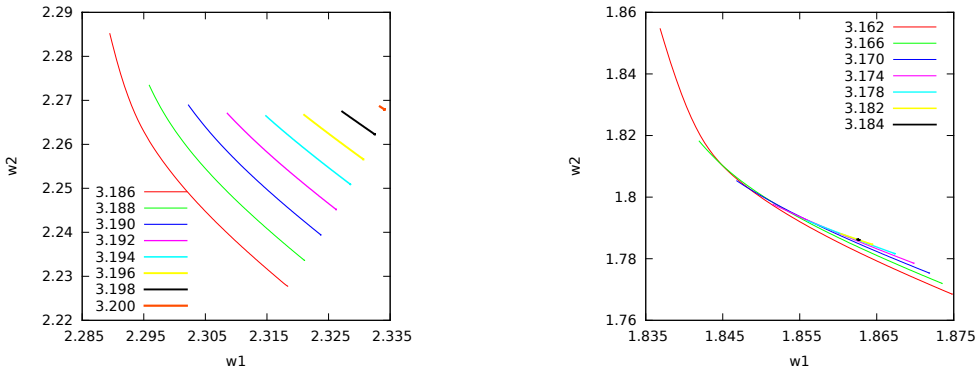

Figure 12. The monotonic relation between in-plane frequency (ω_1) and out-off-plane freuqency (ω_2) of Lissajous orbits for Earth–Moon L_1 point (left) and L_2 (right).

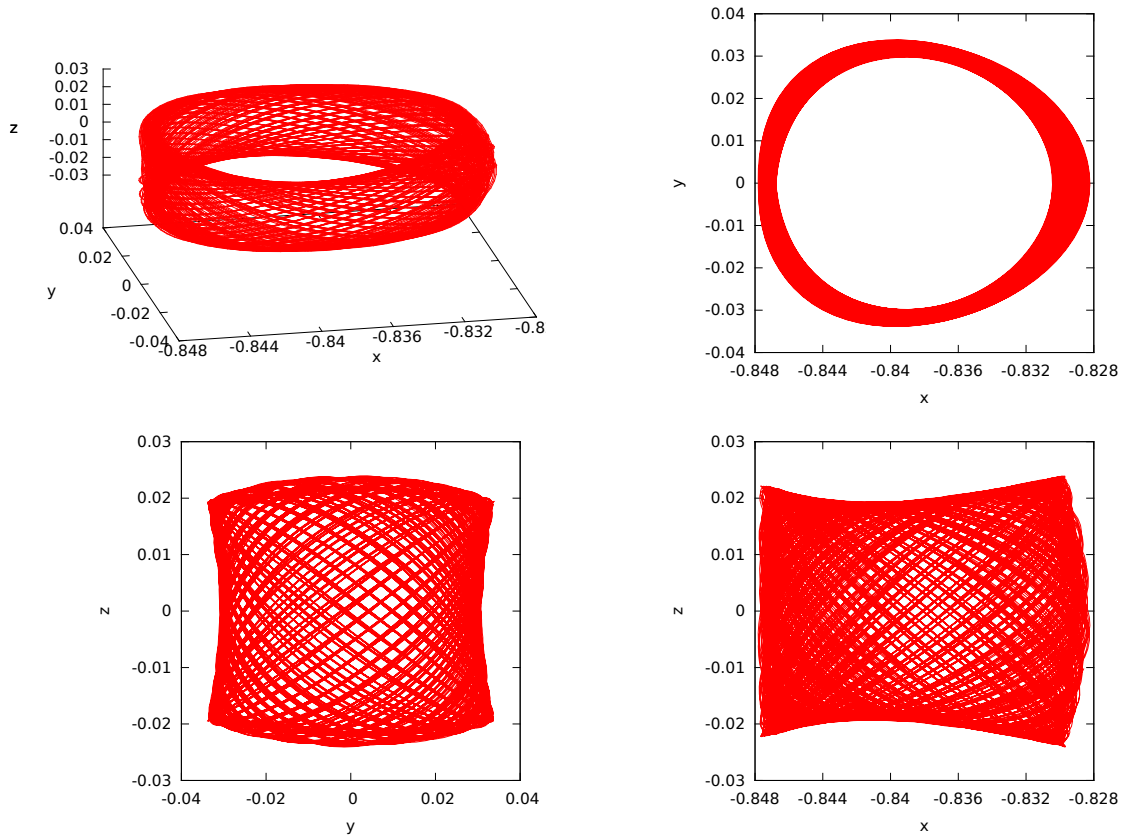

Figure 13. Refinement of a L_1 Lissajous orbit with $\alpha = 0.0579999987$, $\beta = 0.1285250065$, and $C_J = 3.194$. Only the segment of the first 10 years of the 60-year orbit is plotted.

mention is that Lissajous orbits around L_1 preserve their geometries well after having been refined for 60 years with the exception of $C_J = 3.200$, while Lissajous orbits around L_2 seem to have "contracted" after the refinement for all the values of Jacobi Constant. This fact, again, shows us the dynamics around Earth–Moon L_2 point is more rich and thus complicated than L_1.

CONCLUSIONS

This paper presents a novel algorithm that is capable of refining large time-span orbits in real ephemeris. The algorithm is an iterative process combining the parallel shooting and the refined Fourier analysis with an initial guess produced in CR3BP. Based on this algorithm, dynamical substitutes of both L_1 and L_2 libration points and the orbits around them, including periodic ones (planar Lyapunov orbits, vertical Lyapunov orbits, and halo orbits) and Lissajous ones, are obtained and analysed for 60 years (100 years for the dynamical substitutes of $L_{1,2}$) in the Earth-Moon system, during which time most of the relavant Sun-Earth-Moon periods are covered. The analysis mainly concerns two aspects: one is the basic frequencies of these orbits; the other is the Poincaré intersections in phase space, both having shown the evidence of strong perturbations from the Sun. All the results obtained contribute to provide insights into the dynamical behaviour of these orbits in real Earth-Moon environment, and will hopefully benefit the future mission design within this realm.

ACKNOWLEDGEMENTS

This work has been supported by the Spanish grants MTM2010–16425 (G.G.), MTM2009–06973, 2009SGR859 (J.J.M.), and Chinese grant NSFC–10702078 (L.Y.). The author Lian Yijun has been awarded a scholarship (No.2011611052) under the State Scholarship Fund of China to pursue his study in Spain as a joint PhD student.

REFERENCES

[1] À. Jorba and J. J. Masdemont, "Dynamics in the Center Manifold of the Restricted Three-Body Problem," *Physica D: Nonlinear Phenomena*, Vol. 132, 1999, pp. 189–213.

[2] G. Gómez and J. M. Mondelo, "The Dynamics Around the Collinear Equilibrium Points of the RTBP," *Physica D: Nonlinear Phenomena*, Vol. 157, No. 4, 2001, pp. 283–321.

[3] G. Gómez, J. J. Masdemont, and C. Simó, "Quasihalo Orbits Associated with Libration Points," *Journal of the Astronautical Sciences*, Vol. 42, No. 2, 1998, pp. 135–176.

[4] M. A. Andreu, "The Quasi-Bicircular Problem," *PhD thesis*, Universitat de Barcelona, 1998.

[5] *Theory of Orbits: The Restricted Problem of Three Bodies*. Academic Press, 1967.

[6] G. Gómez, J. M. Mondelo, and C. Simó, "A Collocation Method for the Numerical Fourier Analysis of Quasi-Periodic Functions. I: Numerical Tests and Examples," *Discrete and Continuous Dynamical Systems - Series B*, Vol. 14, No. 1, 2010, pp. 41–74.

[7] G. Gómez, J. M. Mondelo, and C. Simó, "A Collocation Method for the Numerical Fourier Analysis of Quasi-Periodic Functions. II: Analytical Error Estimates," *Discrete and Continuous Dynamical Systems - Series B*, Vol. 14, No. 1, 2010, pp. 75–109.

[8] G. Gómez, J. J. Masdemont, and J. M. Mondelo, "Solar System Models with a Selected Set of Frequencies," *Astronomy & Astrophysics*, Vol. 390, No. 2, 2002, pp. 733–749.

[9] X. Y. Hou and L. Liu, "On Quasi-Periodic Motions Around the Triangular Libration Points of the Real EarthMoon System," *Celestial Mechanics and Dynamical Astronomy*, Vol. 110, No. 1, 2011, pp. 71–98.

[10] *Methods of Astrodynamics*. Wiley, 1968.

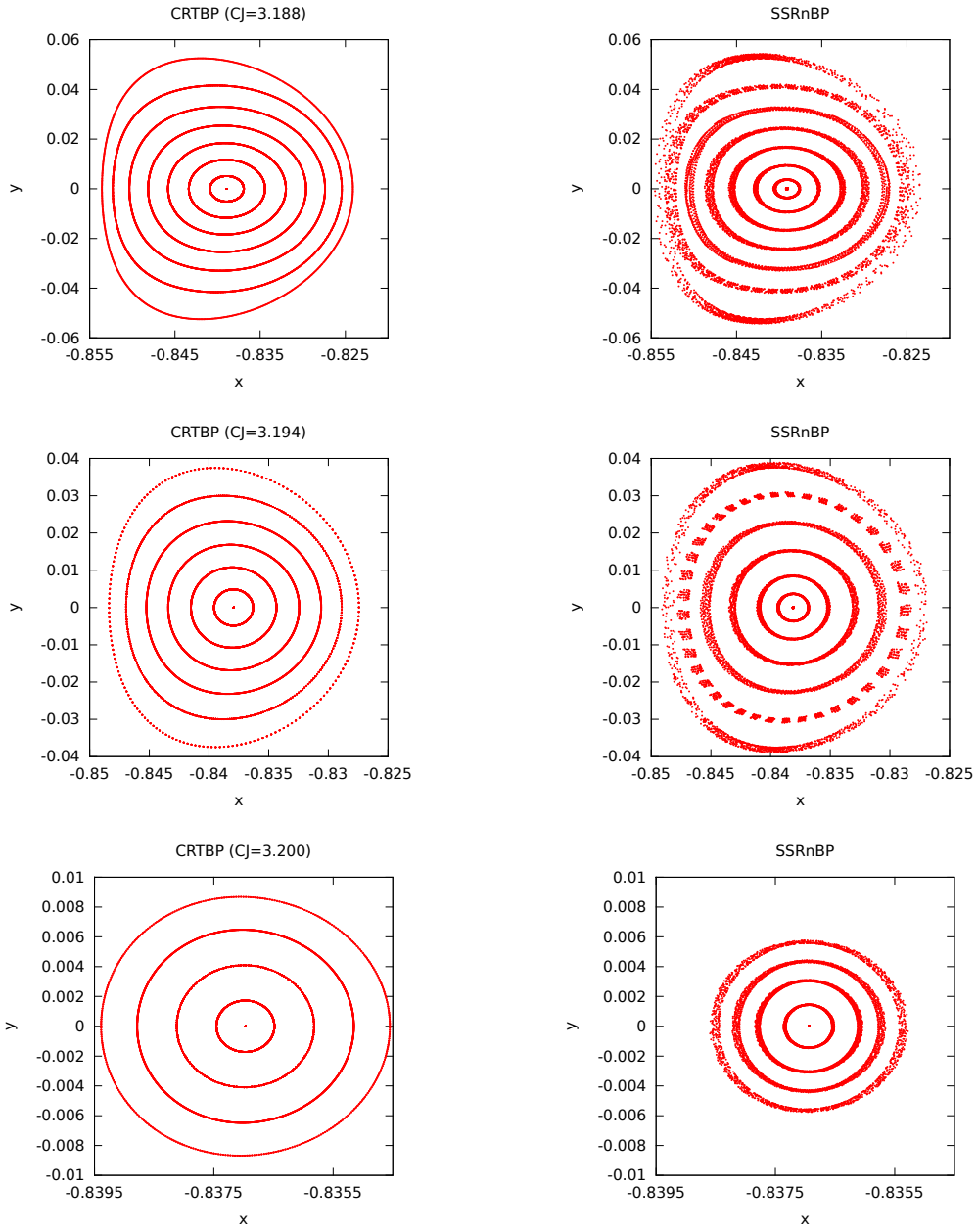

Figure 14. Poincaré map representation with $\{z = 0, \dot{z} > 0\}$ of the Lissajous+Lyapunov orbits around the L_1 point of the Earth–Moon system. On the left hand side, we represent the intersections of the orbits computed in the CR3BP model, and on the right hand side the intersections of the refined trajectories in the full Solar System model (SSRnBP).

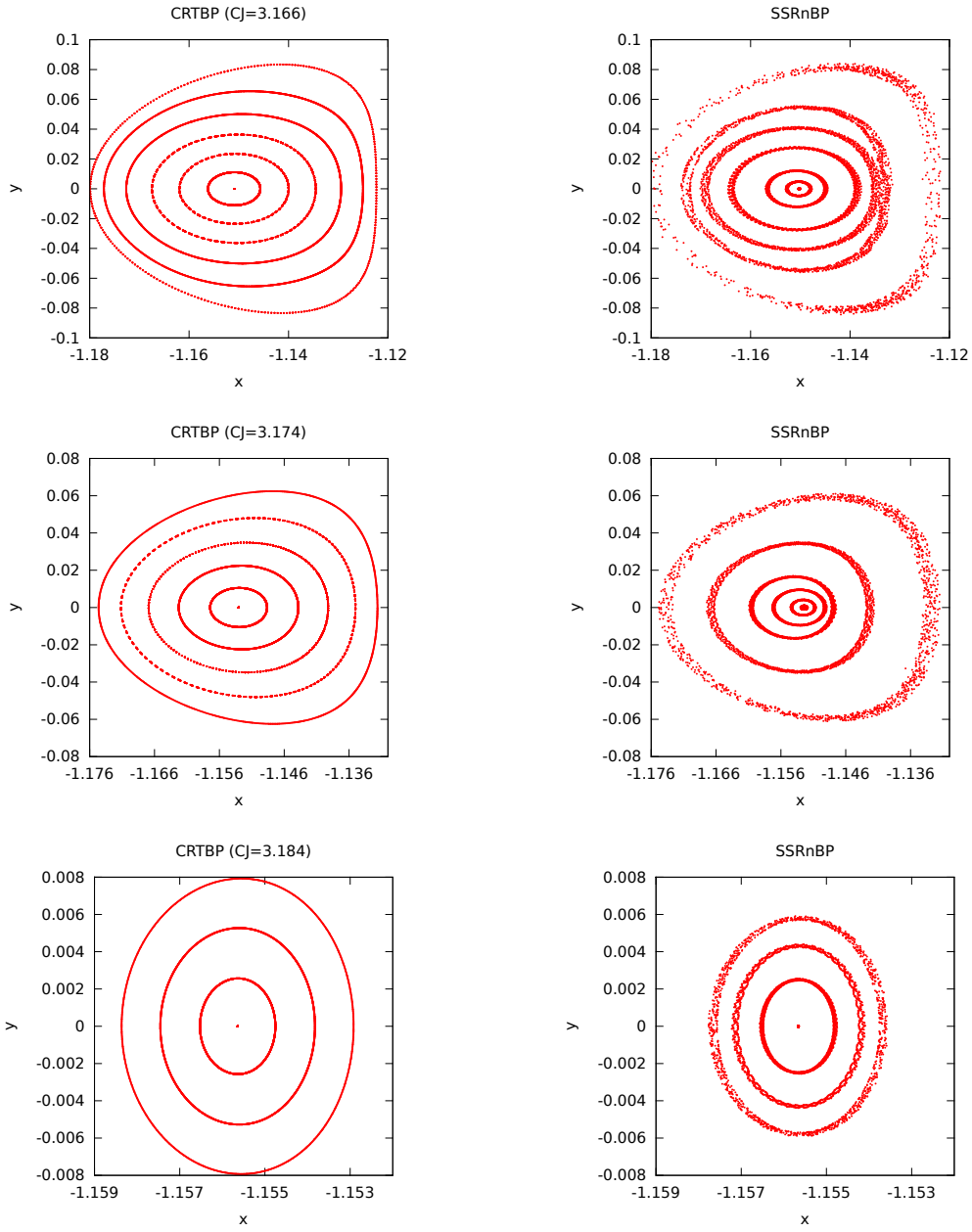

Figure 15. Poincaré map representation with $\{z = 0, \dot{z} > 0\}$ of the Lissajous+Lyapunov orbits around the L_2 point of the Earth–Moon system. On the left hand side, we represent the intersections of the orbits computed in the CR3BP model, and on the right hand side the intersections of the refined trajectories in the full Solar System model (SSRnBP).